Demonstration of 192 Gbps Single-Carrier PDM-16QAM W-band Wireless Delivery over 4600 meters

Weiping Li(1), Jianjun Yu (1)*, Xianmin Zhao(2), Jiaxuan Liu(1), Yi Wei(1), Tianqi Zheng(1), Mingxu Wang(1), Xiaoxue Ji(1), Kaihui Wang(1), Wen Zhou(1), and Feng Zhao(3)

(1) Fudan University, Shanghai, 200433, China * jianjun@fudan.edu.cn
(2) Harbin Institute of Technology, Harbin, China, 150001
(3) Xi'an University of Posts and Telecommunications, Xi'an, 710121, China

Abstract: *we experimentally demonstrate a high-speed long-haul wireless transmission link at W-band can realize up to 192Gbps wireless delivery over 4600 meters with a BER less than 2.4×10^{-2}.*

Introduction

The exponential expansion of information in today's world has presented significant difficulties for the transmission capacity of current communication systems. In response to this challenge, researchers have turned to the W-band (75-110GHz) as a potential solution. The W-band offers a wider bandwidth and relatively small atmospheric loss, making it an attractive option for high-speed wireless data transmission. Photonics-aided technology [9-13] has been applied in W-band mm-wave communication system to effectively resist the bandwidth limitation and electromagnetic interference of electronic equipment, which can also effectively promote the seamless integration of wireless and fiber-optic networks.

How to realize the long-haul transmission of ultra-bandwidth and large-capacity mm-wave signals is one of the key means to effectively meet the demand of the mobile backhauling and emergency communications. Experimentally demonstrated 100-Gbps and 400-Gbps wireless signal delivery at W-band were reported adopting photonic mm-wave generation, but the wireless transmission distance is no more than 2m [14-15]. It is evident that, however, several meters or even tens of meters of wireless transmission distance cannot effectively meet the aforementioned application demand. Based on single-carrier modulation scheme, 80-Gbps wireless signal delivery over 300m [16], 20-Gbps wireless signal delivery over 1700m [17], 54-Gbps wireless signal delivery over 2500m [18], and 91.6-Gbps wireless signal delivery over 4600m [19] at W-band have been demonstrated. But the aforementioned demonstrations [16-19] has relatively low wireless transmission rate or short wireless transmission distance, which need to be further improved.

In this paper, we experimentally demonstrate a high-speed long-haul W-band wireless transmission system can realize up to 192-Gbps wireless delivery over 4600m at 87.5-GHz with a BER less than 2.4×10^{-2}. The product of the transmission distance and the bit rate is 883.2 Gbps*km, which is a new record number for optical-wireless integration transmission to the best of our knowledge. Compared with our previous work with single-carrier delivery [16-19], the newly adopted ultra-bandwidth high-gain W-band power amplifiers (PA1 and PA2) and low noise amplifiers (LNA1 and LNA2) at the transmitter end significantly promotes the data rate improvements. In addition, we not only simplify the offline DSP algorithm by employing traditional single-input single-output (SISO) second-order Volterra equalizer to replace the complex multiple-input and multiple-output (MIMO) Volterra equalizer [19], but also increase the wireless rate by 84% while keeping the wireless distance unchanged, which are crucial to reduce system cost and power consumption for practical deployment of the upcoming high-speed B5G and 6G wireless communication.

Experimental setup

The experimental setup for high-speed long-haul mm-wave wireless transmission system is depicted in Fig.1(a). Continuous waves of 1550 nm and 1550.7 nm are emitted by two free-running external cavity lasers (ECL1 and ECL2) with a linewidth of less than 100kHz and a typical frequency stability of ±0.3 GHz for 24 hours. The I/Q modulator (3dB bandwidth of 40 GHz), is driven by the 13 dBm CWs emitted from ECL1. In the Tx-side DSP, a raised-cosine (RC) filter with a roll-off factor of 0.01 is applied to the generated QAM symbols to resist the bandwidth limitation of photoelectric devices. We use an arbitrary waveform generator (AWG) with 120-GSa/s sampling rate to generate the baseband electrical signals. After being generated by the AWG, the I-th and Q-th analog electrical signals undergo amplification through a pair of parallel electric

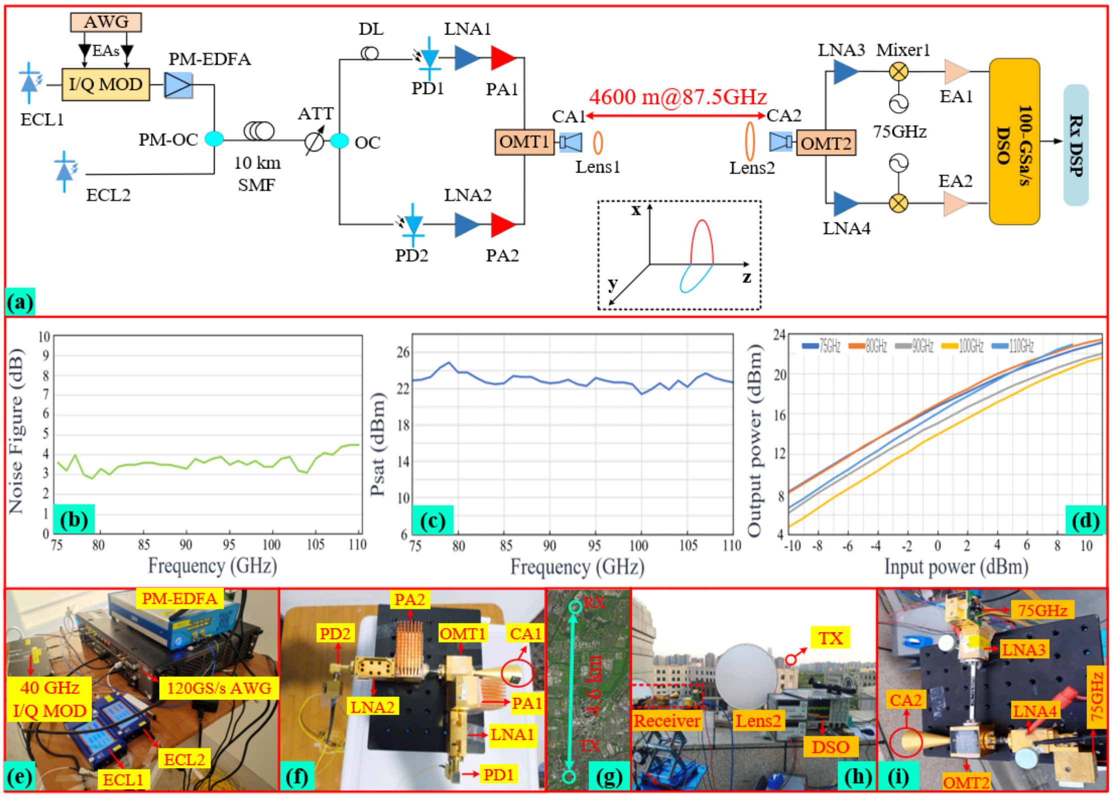

Fig. 1 (a) The experimental setup of the photonics-aided W-band polarization multiplexing communication system; (b) Noise figure vs. Frequency for LNA1 and LNA2; (c) Psat vs. Frequency for LNA1 and LNA2; (d) Output power vs. Input power for PAs; (e)-(f) The scenes of the transmitter side; (g) The map display of the 4.6 km wireless communication link; (h)-(i) The scenes of the receiving side of the wireless link;

amplifiers (EAs) with a 25 dB gain. These amplified signals are then fed into the I/Q modulator for modulation. A PM-OC couple the 10 dbm CWs, emitted from ECL2 with the optical signals ,which is amplified by a PM-EDFA to compensate for the insertion loss of the modulator. After 10 km SMF-28 transmission, the optical signals enter into base station, in which an optical attenuator (ATT) undertakes the function of changing the input optical power conveniently. Next, an optical coupler (OC) is used to divide the optical signals into two paths. The signals in one of the paths pass through an optical delay line (DL, ~100m SMF-28), which can eliminate the correlation between two paths by providing a delay of more than 1000 symbols. Then the 87.5 GHz mm-wave signals in H- and V-polarization direction are generated via two separate photodiodes (PD1 and PD2) with 3-dB bandwidth of 100 GHz. The cascaded LNA1 and PA1 are used to amplify the electrical mm-wave from PD1. Identically, the cascaded LNA2 and PA2 are used to amplify the electrical mm-wave from PD2. The LNA1 and LNA2 have a 35-dB gain and 3.5 dB noise figure at 87.5 GHz, while the PA1 and PA2 have 23-dBm saturation output power (Psat) at 87.5 GHz. Fig.1(b) shows the noise figure performance of LNA1 and LNA2. Fig. 1(c-d) show the Psat and output power curve of PAs, respectively. The two signals output from PAs are combined together by a W-band orthomode transducer (OMT1) with 35-dB isolation between the H- and V-pol directions.

Then, the dual-polarized mm-wave are transmitted to the wireless space through the combination of conical antenna (CA1) and Lens1 with a gain of 34dBi. Fig.1(e-f) display the scenes of the transmitter side. Fig.1(g) shows the map display of the 4600 m wireless communication link. At the receiving side of the wireless link, the combination of CA2 and Lens2 with a gain of 56dBi is used to receive mm-wave signals. Subsequently, the received signals are divided into the H-polarized and V-polarized signals by OMT2. The H-polarized and V-polarized signals are amplified by LNA3 and LNA4 with 30dB gain, respectively. They are then down-converted by mixers driven by 75 GHz RF sources to generate 12.5 GHz intermediate frequency (IF) signals, respectively. Before being captured by the digital storage oscilloscope (DSO), the IF signals are amplified by EAs with a gain of 35 dB. Fig.1(h)-(i) display the scenes of the receiving side of the wireless link. The offline DSP at the receiving side includes down-conversion, resampling, clock recovery, chromatic dispersion (CD) compensation, T/2 constant modulus algorithm (CMA), frequency offset estimation (FOE), blind

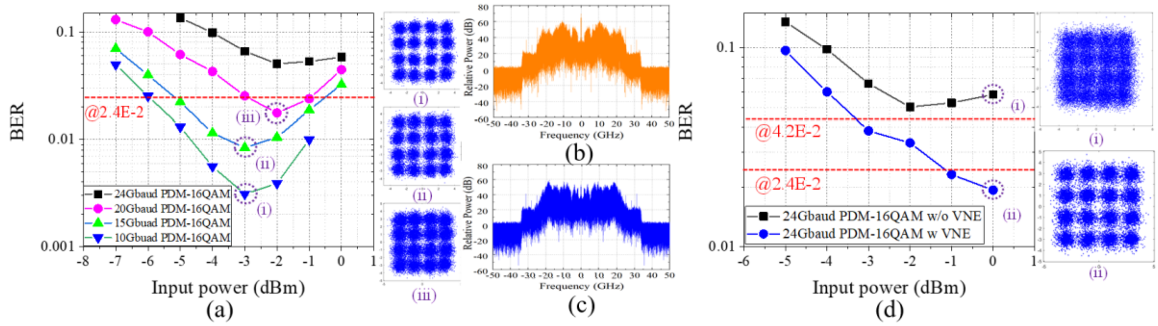

Fig. 2: (a) BER of PDM-16QAM signals vs. the input optical power of PDs; (b)The electrical spectra of the sampled X-polarized 24Gbaud signals; (c) The electrical spectra of the sampled Y-polarized 24Gbaud signals; (d) BER of 24 Gbaud PDM-16QAM signals with and without volterra nonlinear equalization.

phase search (BPS) algorithms, and decision-driven Least Mean (DD-LMS) equalizer.

Results and Discussion

The four curves in Fig.2(a) show the BER versus input power of PDs for 10~24 Gbaud PDM-16QAM signals. Due to the increase of the signals baud rate, the requirement for the system bandwidth increases, which leads to the deterioration of BER performance. In addition, the BER of signals with different baud rate decreases as the input power of PDs increases from -7 dBm to -3 dBm due to the increase in signals to noise ratio (SNR). However, when the input power of PDs increases from -2 dBm to 0 dBm, the BER of signals increases instead because the PAs and LNAs are affected by the saturation effect. Therefore, the BER curves depicted in Fig.2(a) all show a trend of first falling and then rising. When the input power is about -3 or -2 dBm, the BER of signals are minumum. The minumum BER of 10, 15, 20, and 24 Gbaud PDM-16QAM signals is 3.1×10^{-3}, 8.4×10^{-3}, 1.75×10^{-2}, and 5.08×10^{-2}, respectively. The insets(i)–(iii) in Fig.2(a) respectively show the recovered signals constellations with 10, 15, 20 Gbaud. Note that the DSP we used at this time is the simple DSP mentioned above, which doesn't take much running time.

Since the BER of 24Gbaud PDM-16QAM signals does not reach below the SD-FEC threshold, we must use further DSP algorithm for processing. In the previous work [19], we used the MIMO volterra nonlinear equalization (VNE) for processing. Although good performance was achieved, it inevitably greatly increased the running complexity of offline DSP, which will increase system cost and power consumption. With the correction of transceiver alignment, the OMTs we used in this system can exhibit up to 35 dB polarization isolation [20]. As a result, the crosstalk between two polarized channels is relatively small. However, the nonlinear effect caused by the saturation effect of amplifiers is unavoidable in the system. We try our best to reduce the complexity of the offline DSP algorithm. Instead of MIMO VNE, we add the SISO VNE to the above-mentioned DSP to further process the 24Gbaud PDM-16QAM signals.

Fig.2(b-c) show the electrical spectra of the sampled X-polarized and Y-polarized 24Gbaud signals after 4600 m wireless delivery, respectively. Fig.2(d) shows the BER performance of 24Gbuad PDM-16QAM signals with (w) SISO VNE and without (w/o) SISO VNE. When the input power of PDs exceeds -2dBm, the BER increases due to nonlinear effects. However, with the help of VNE, the influence of nonlinear effects on signals is well eliminated, thereby continuing to reduce the BER. As a result, the BER of the 24Gbaud PDM-16QAM signals with VNE shows a continuous downward trend. When the input power of PDs exceeds -1dBm, the BER is below the 15% SD-FEC threshold of 2.4×10^{-2}. Therefore, the maximum data rate of the system is 24×2×4=192 Gbps. If removing the 15% SD-FEC overhead, the maximum net rate is 24×2×4/(1+15%)=167 Gbps.

Conclusions

We experimentally demonstrate a high-speed long-haul W-band wireless transmission system can realize up to 192-Gbps wireless delivery over 4600m at 87.5-GHz with a BER less than 2.4×10-2. The ultra-bandwidth high-gain W-band PAs and LNAs at the transmitter end significantly promotes the data rate improvements. Furthermore, in conjunction with the alignment of the transceiver system, we simplify the DSP to reduce system cost and power consumption for practical deployment of the high-speed B5G and 6G wireless communication.

Acknowledgements

This work was partially supported by the NNSF of China with grant number of 61720106015 and 62127802.

References

[1] E. Forestieri, M. Secondini, L. Potì and F. Cavaliere, “High-Speed Optical Communications Systems for Future WDM Centralized Radio Access Networks,” Journal of Lightwave Technology. vol. 40, no. 2, pp. 368-378, 2020.

[2] Y. Xu, E. Agrell, and M. Brandt-Pearce, “Cross-layer static resource provisioning for dynamic traffic in flexible grid optical networks,” Journal of Optical Communications and Networking. vol. 13, no. 3, pp. 1-13, 2021.

[3] C. Yeh, H. Ko, S. Liaw, L. Liu, J. Chen and C. Chow, “A Survivable and Flexible WDM Access Network by Alternate FSO- and Fiber-Paths for Fault Protection,” Photonics Journal, vol. 14, no. 1, pp. 1-5, 2022.

[4] H. Chung, H. Lee, K. Kim, K. Doo, Y. Ra, and C. Park, “Optical Access Networks for Tactile Internet Services,” Photonic Networks and Devices, NeM1C. 4, 2021.

[5] H. Chung, H. Lee, K. Kim, K. Doo, Y. Ra, and C. Park, “Optical Access Networks for Tactile Internet Services,” Photonic Networks and Devices, NeM1C. 4, 2021.

[6] M. Gay, A. O’Hare, L. Bramerie, Z. Hao, S. Fresnel, C. Peucheret, P. Besnard, S. Joshi, S. Barbet, and F. Lelarge, “Single Quantum Dash Mode-Locked Laser as a Comb-Generator in Four-Channel 112 Gbit/s WDM Transmission,” in Optical Fiber Communication Conference, Tu2H.5, 2014.

[7] X. Zhu, C. Wang, J. Huang, M. Chen and H. Haas, “A Novel 3D Non-Stationary Channel Model for 6G Indoor Visible Light Communication Systems,” in IEEE Transactions on Wireless Communications, doi: 10.1109/TWC.2022.3165569.

[8] P. Ossieur, H. Ramon, J. Lambrechts, M. Vanhoecke, L. Breyne, S. Zhou and J. Bauwelinck. “Electronic ICs for Silicon Photonic Transceivers,” In IEEE 15th International Conference on Group IV Photonics (GFP) (pp. 1-2), 2018.

[9] S. Ishimura, T. Fukui, R. Tanomura, G. Soma, Y. Nakano, and T. Tanemura, “64-QAM Self-Coherent Transmission Using Symmetric Silicon Photonic Stokes-Vector Receiver,” in Optical Fiber Communication Conference, M4J.6, 2022.

[10] K. Powell, A. Shams-Ansari, S. Desai, M. Austin, J. Deng, N. Sinclair and X. Yi. “High-Q suspended optical resonators in 3C silicon carbide obtained by thermal annealing,” Optics express, vol. 28, no. 4, pp.4938-4949, 2020.

[11] Z. Cao, X. Zhang, G. Osnabrugge, J. Li, I. Vellekoop and A. Koonen. (2019). “Reconfigurable beam system for non-line-of-sight free-space optical communication”. Light: Science & Applications. vol. 8, no. 1, pp.1-9, 2019.

[12] A. Delmade, E. Martin, C. Browning and L. Barry, “5G Millimeter-Wave Analog RoF System employing Optical Injection Locking and Direct Modulation of DFB Laser,” in Optical Fiber Communication Conference, W4C.7, 2022.

[13] G. Carpintero, Y. Yoshida, and J. Azaña, “Editorial Special Issue on Microwave Photonics,” Journal of Lightwave Technology. vol. 39, no. 24, pp. 7549-7550, 2021.

[14] X. Li, J. Yu, J. Zhang, F. Li, and J. Xiao, “Antenna polarization diversity for 146Gb/s polarization multiplexing QPSK wireless signal delivery at W-band,” Proc. OFC 2014, San Francisco, California, M3D.7.

[15] J. Yu, X. Li, J. Zhang, and J. Xiao, “432-Gb/s PDM-16QAM signal wireless delivery at W-band using optical and antenna polarization multiplexing,” Proc. ECOC 2014, Cannes, France, We.3.6.6.

[16] X. Li, J. Yu, J. Xiao, Z. Zhang, Y. Xu, and L. Chen, “Field trial of 80-Gb/s PDM-QPSK signal delivery over 300-m wireless distance,” Proc. OFC 2015, Los Angeles, CA, Th5A.5.

[17] J. Xiao, J. Yu, X. Li, Y. Xu, Z. Zhang, and L. Chen. “20-Gb/s PDM-QPSK Signal Delivery over 1.7-km Wireless Distance at W-Band,” in Optical Fiber Communication Conference, W4G.4, 2015.

[18] X. Li, J. Yu, K. Wang, Y. Xu, L. Chen, L. Zhao, and W. Zhou. “Delivery of 54-Gb/s 8QAM W-Band Signal and 32-Gb/s 16QAM K-Band Signal Over 20-km SMF-28 and 2500-m Wireless Distance,” Journal of Lightwave Technology. vol. 36, no. 1, pp. 50-56, 2018.

[19] F. Wang, J. Yu, Y. Wang, W. Li, B. Zhu, J. Ding, K. Wang, C. Liu, C. Wang, M. Kong, L. Zhao, F. Zhao, and W. Zhou. “Delivery of polarization-division-multiplexing wireless millimeter-wave signal over 4.6-km at W-band,” Journal of Lightwave Technology. vol. 40, no. 19, pp. 6339-6346, 2022.

[20] Y. Cai, M. Zhu, J. Zhang, M. Lei, B. Hua, Y. Zou, W. Luo, S. Xiang, L. Tian, J. Ding, L. Ma, Y. Huang, J. Yu, and X. You, "Real-time 100-GbE fiber-wireless seamless integration system using an electromagnetic dual-polarized single-input single-output wireless link at the W band," Opt. Lett, vol. 48, pp. 928-931, 2023.